HHS Public Access

Author manuscript

Clin Cancer Res. Author manuscript; available in PMC 2020 March 01.

Published in final edited form as:

Clin Cancer Res. 2019 September 01; 25(17): 5351–5363. doi:10.1158/1078-0432.CCR-18-4192.

Dissecting the stromal signaling and regulation of myeloid cells and memory effector T cells in pancreatic cancer

Alex B Blair[1,2,3], **Victoria M Kim**[1,2,3], **Stephen T Muth**[1,2], **May Tun Saung**[1,2,4], **Nathalie Lokker**[5], **Barbara Blouw**[6], **Todd D Armstrong**[1,2], **Elizabeth M Jaffee**[1,2,4], **Takahiro Tsujikawa**[7,8,9], **Lisa M Coussens**[8,9], **Jin He**[1,2,3], **Richard A Burkhart**[1,2,3], **Christopher L Wolfgang**[1,2,3,4], **Lei Zheng**[1,2,3,4]

[1]The Sydney Kimmel Comprehensive Cancer Center, Johns Hopkins University School of Medicine, Baltimore, MD

[2]The Pancreatic Cancer Precision Medicine Center of Excellence Program, Johns Hopkins University School of Medicine, Baltimore, MD

[3]Department of Surgery, Johns Hopkins University School of Medicine, Baltimore, MD

[4]Department of Oncology, Johns Hopkins University School of Medicine, Baltimore, MD

[5]AstraZeneca, Gaithersburg, MD

[6]Halozyme Therapeutics, Inc., San Diego, CA

[7]Department of Otolaryngology, Head and Neck Surgery, Kyoto Prefectural University of Medicine, Kyoto, Japan

[8]Department of Cell, Developmental & Cancer Biology, Oregon Health and Science University, Portland, OR

[9]Knight Cancer Institute, Oregon Health and Science University, Portland, OR

Abstract

Purpose: Myeloid cells are a prominent immunosuppressive component within the stroma of pancreatic ductal adenocarcinoma(PDAC). Previously, targeting myeloid cells has had limited success. Here, we sought to target the myeloid cells through modifying a specific stromal component.

[*]**Corresponding Author:** Lei Zheng, M.D., Ph.D., 1650 Orleans Street, CRB1 Room 488, Baltimore, MD 21042, Tel: 410-502-6241, Fax: 410-614-8216, lzheng6@jhmi.edu.

Author contributions: ABB, VK, NL and LZ designed the research studies. ABB, VK, SM, BB, and TT conducted experiments. ABB, VK, BB, TT and LZ acquired data. ABB, VK, TDA, LZ analyzed data. All authors critically reviewed the manuscript

Conflict of interests: LZ receives grant supports from Bristol-Meyer Squibb, Merck, iTeos, Amgen, Gradalis, NovaRock, and Halozyme. EMJ receives research funding from Roche and Aduro Biotech. EMJ and LZ received the royalty for licensing GVAX to Aduro Biotech. LZ is a paid consultant at Biosynergies, Merck, NovaRock, Foundation Medicine, Oncorus, Alphamab (stock owner), Mingruizhiyao (stock owner), and AstroZeneca. BB is an employee of Halozyme Therapeutics. NL is a former employee of Halozyme Therapeutics. LMC declares that she is a paid consultant for Cell Signaling Technologies and received reagent support from Plexxikon, Inc., Pharmacyclics, Inc., Acerta Pharma, Jansen R&D, Deciphera Pharmaceuticals, Genentech, Inc., Aduro Biotech., Eisai Inc., Abbott Labs, Roche Glycart AG, and NanoString Technologies. LMC is a member of the Scientific Advisory Boards of Syndax Pharmaceuticals, Inc., Carisma Therapeutics, Verseau Therapeutics, Inc., and Zymeworks Inc. ABB, VK, SM, MTS, TDA, TT, JH, RAB, CLW have no relevant conflict of interests to report.

Experimental Design: A murine model of metastatic PDAC treated with an irradiated whole cell PDAC vaccine and PDAC specimens from patients treated with the same type of vaccine were used to assess the immune-modulating effect of stromal hyaluronan (HA) degradation by PEGPH20.

Results: Targeting stroma by degrading HA with PEGPH20 in combination with vaccine decreases CXCL12/CXCR4/CCR7 immunosuppressive signaling axis expression in cancer-associated-fibroblasts, myeloid, and $CD8^+$ T-cells, respectively. This corresponds with increased CCR7(–) effector memory T-cell infiltration, an increase in tumor specific IFNγ, and improved survival. In the stroma of human PDACs treated with the same vaccine, decreased stromal CXCR4 expression significantly correlated with decreased HA and increased cytotoxic activities, suggesting CXCR4 is an important therapeutic target.

Conclusions: This study represents the first to dissect signaling cascades following PDAC stroma remodeling via HA depletion, suggesting this not only overcomes a physical barrier for immune cell trafficking, but alters myeloid function leading to downstream selective increases in effector memory T-cell infiltration and anti-tumor activity.

Keywords

Stroma; Myeloid; Hyaluronic Acid; CXCR4; PEGPH20; Hyaluronidase; Immunotherapy

INTRODUCTION

Pancreatic adenocarcinoma (PDAC) is an aggressive malignancy broadly resistant to current treatment modalities. There is a distinct demand for the development of novel therapeutic approaches such as immunotherapy. Cancer immunotherapy has been a monumental advancement over the last decade for the treatment of many disease biologies(1–4). Unfortunately, single agent immunotherapy treatment, such as checkpoint inhibitors, have failed to show efficacy in PDAC (4,5). While the infiltration of effector $CD8^+$ T-cells may confer survival benefit and is predictive of a beneficial response to immunotherapy, their presence is rare while immunosuppressive myeloid cells dominate the PDAC tumor microenvironment (TME)(6–8). PDAC classically elicits an intense desmoplastic reaction including a well-developed stromal component comprising as much as 90% of tumor mass in both primary and metastatic disease(9,10). This stroma serves as an impenetrable physical barrier limiting therapeutic access as well as forming a complex signaling axis between neoplastic and stromal cells. This network of signals regulates cancer growth, manipulates immune surveillance and limits the efficacy of both classic chemotherapy and immunotherapy(9–11). However, the role of stromal depletion in PDAC is controversial, as prior studies reported an acceleration of cancer progression following the reduction of cancer associated fibroblasts (CAF) via the hedgehog signaling pathway(12,13).

Although broad depletion of stroma may fundamentally inhibit immunosurveillance, targeting a specific stromal component may still yield antitumor immune-modulating effects. Hyaluronan (HA) is an extracellular glycosaminoglycan component of tissues that binds to proteoglycans and other hyadherins forming a complex network in the extracellular matrix(14,15). Accumulation of HA occurs in many human tumors and is predictive of more

aggressive disease and treatment resistance(15,16). HA is abundant in the desmoplastic stromal component of PDAC and thus hypothesized to significantly contribute to the pro-tumorigenic impact of the TME and its ability to prevent maximal chemotherapeutic drug accumulation(15–17). HA accumulation is associated with a parallel increase in collagen, α-SMA expression, and proteoglycans, all together cooperating to form a complex, tumor-promoting TME(18). Thus, HA is an attractive therapeutic target. PEGPH20 is a PEGylated recombinant human PH20 hyaluronidase developed to degrade HA following its systemic administration. Depletion of HA through hyaluronidase diminishes collagen synthesis, depletes chondroitin sulfates and remodels the tumor stroma(18–22). The accumulation of HA in untreated PDAC is typically associated with elevated interstitial fluid pressure exceeding typical arteriolar and capillary pressures, thus serving as a major impediment to therapeutic access. Following systemic dosing of PEPGH20, interstitial fluid pressure significantly decreased and a corresponding significant increase in the percentage of $CD31^+$ vessels with discernable, patent lumens was appreciated, although without a change in the total vessel number. Furthermore, after PEGPH20 dosing, a significant increase in drug delivery, as noted by doxorubicin fluorescence intensity, was appreciated, further suggesting a restoration of functional perfusion and unimpeded therapeutic access(19). The reduction of tumor HA thereby improves vascular perfusion, diminishes hypoxia, and increases chemotherapy penetration and dispersion(18,22–24). This concept was supported with initial phase 1b and 2 studies showing safety and improved efficacy of PEGPH20 in combination with standard chemotherapeutics, Gemcitabine and nab-paclitaxel, lengthening progression-free survival in PDAC patients(25,26). However, the role of PEGPH20 in enhancing the efficacy of chemotherapy was questioned by another phase 2 study showing that the FOLFIRINOX chemotherapy in combination with PEGPH20 was inferior to FOLFIRINOX alone for metastatic PDAC patients(27). The difference in the results of two PEGPH20 studies may be explained by different chemotherapy regimens used in combination with PEGPH20 or different schedules of PEGPH20 used in different clinical trials. Nevertheless, the potential role of PEGPH20 in facilitating the intratumoral infiltration of immune cells is still intriguing. One study demonstrated that PEGPH20 enhanced NK cell infiltration, antibody delivery and antibody-dependent cell-mediated cytotoxicity in preclinical models of various solid tumors(28). Manuel *et al.* reported that PEGPH20 in combination with shIDO-ST, a salmonella based therapy targeting indolemaine 2,3-dioxygenase, resulted in an increased infiltration of anti-tumor polymorphonuclear neutrophils leading to reduced PDAC tumor burden in mice(23). While not exclusively targeting HA, Elahi-Gedwillo *et al.* reported that general inhibition of fibrotic activity by Halofuginone treatment altered the PDAC TME leading to an increase in the infiltration of inflammatory macrophages and cytotoxic $CD8^+$ T-cells, with the greatest immune infiltration observed in regions of low HA(24). Nevertheless, whether targeting HA can modulate the function of tumor infiltrating immune cells has not been addressed.

Myeloid cells are a prominent cell type within the pancreatic stroma(29). These cells are known to be predominately immunosuppressive in PDAC via a myriad of signals contributing to the paucity of infiltrating anti-tumor effector immune cells(29–31). Targeting the myeloid cells has been challenging with growing efforts to manipulate their function by targeting tumor-promoting signaling cascades, such as CXCR2, in order to enhance T-cell

infiltration, inhibit metastases and improve survival(7,32). Another notable signaling cascade target is the CXCR4 pathway. CXCR4 is most prominently recognized for its role as a co-factor required for entry of the HIV virus into $CD4^+$ T-cells, however, it is also a commonly overexpressed chemokine receptor in multiple human malignancies (33,34). This pathway has previously been shown to polarize the TME towards a more immunosuppressive nature by increasing myeloid-derived suppressor cell (MDSC) recruitment and promoting tumor progression and growth (35–37). The development of a therapeutic antibody targeting a G-protein coupled receptor such as CXCR4 has been challenging. Inhibition of CXCR4 with small molecular drugs such as AMD3100 has shown significant benefit in preclinical models of PDAC and has been associated with increased $CD8^+$ T-cell infiltration and tumor volume regression(38); however, the clinical feasibility and translatability of applying AMD3100 for cancer treatment remains questionable. Nevertheless, clinical trials with CXCR4 inhibition have largely shown limited benefit for PDAC, potentially due to the broad expression of CXCR4 across multiple cell types other than stromal myeloid cells. The inhibition of myeloid cells has so far similarly demonstrated limited benefit in PDAC, thus highlighting the importance of developing therapeutic agents that are able to modulate the function of myeloid cells instead of blocking or depleting them. Previously, it was shown that depleting stromal fibroblasts by targeting fibroblast activation protein-α (FAP) enhances antitumor immunity(39). It is therefore of interest to consider targeting the myeloid cells through modifying a specific stromal component.

In this study, we investigate the role of HA and its targeted depletion by PEGPH20, an agent that is being tested clinically in combination with chemotherapy in the late drug development phase, in modulating the functions of myeloid cells and T-cells in the setting of induced T-cell infiltration by vaccine immunotherapy in both a murine PDAC model and treated human PDAC specimen. We demonstrate that targeting HA can modulate myeloid cell function through inhibiting the CXCR4-mediated signaling axis and subsequently lead to a quantitative increase of T-cell infiltration with a specific rise of intratumoral effector memory T-cells in PDAC.

MATERIALS AND METHODS

Cell lines

KrasLSL.G12D/$^+$; p53R172H/$^+$; PdxCretg/$^+$ (KPC) tumor cells are a previously established PDAC cell line derived from a C57Bl/6 background mouse model utilizing *cre* recombinase under the control of the pancreas-specific pdx-1 promoter and floxed $KRAS^{G12D}$ in combination with mutated p53 ($Trp53^{R172H/+}$) expression(40). They were developed and cultured as previously described(40,41). The cell lines were validated by short-tandem-repeat profiling and tested for mycoplasma every 6 months. B78H1-GM cells are an MHC class I-negative variant of the B16 melanoma tumor, engineered to secrete GM-CSF and utilized in the formulation of the whole cell autologous GVAX vaccine(37).

Mice and in vivo experiments

C57Bl6 female mice (6–8 weeks) were purchased from Harlan Laboratories (Frederick, MD) and maintained in accordance with the Institutional Animal Care and Use Committee

(IACUC) guidelines. Mice considered to have reached a “survival endpoint” including hunched posture, lethargy, dehydration and rough hair coat were euthanized. The IACUC mouse protocol was maintained by third-party management.

The hemispleen technique of tumor inoculation was performed on Day 0 as previously described in details in a video journal(42). In brief, a left subcostal incision is made, the spleen is eviscerated from the mouse, clipped and hemisected. One half of the spleen is injected with 2×10^5 KPC cells resuspended in a volume of 100μl and flushed with 150μl phosphate buffered saline (PBS) in the same syringe. Cells are injected slowly into the exposed hemispleen keeping the syringe upright at all times to avoid spillage of cells. The splenic vessels are then clipped and the injected hemispleen resected to remove residual tumor cells. Following this procedure, diffuse liver metastases are developed (Supplemental Figure 1) and all untreated mice die in 4–6 weeks(42,43).

PEGPH20 was provided by the Halozyme Therapeutics, Inc. formulation group and was generated by conjugating recombinant human hyaluronidase as previously described(20). PEGPH20 (40μg/kg) was administered intravenously (IV) by tail vein injection on Day 6 following surgery. A single low dose of cyclophosphamide (Cy) (100mg/kg; Bristol-Myers Squibb, New York NY) was administered on Day 6 for regulatory T-cell depletion as previously reported(44,45). The human whole cell granulocyte macrophage colony-stimulating factor (GM-CSF) secreting PDAC vaccine (GVAX) composed of allogeneic PDAC tumor cell lines engineered to secrete GM-CSF, was utilized for treatment(46). Cultured KPC and B78H1-GM cells were harvested and combined at an equal concentration of 2×10^7/mL of each cell type. This whole cell combination was irradiated at 50 Gy and administered subcutaneously in three limbs on Day 7. Mice were monitored daily for survival analysis and euthanized by CO_2 inhalation if IACUC approved criteria was met. For $CD8^+$ T-cell depletion, anti-CD8a antibody (10mg/kg IP; 2.43, BioXcell) was started on day 3 following the hemispleen procedure, and administered IP twice weekly until day 30. IgG isotype control (10mg/kg IP; LTF2, BioXcell) was given to the other treatment groups.

For investigation of murine HA expression both the hemispleen technique as well as orthotopic implantation of $1mm^3$ of KPC tumor directly into the mouse pancreas were performed. At 24 hours, 72 hours, 7 days, and 14 days following PEGPH20 treatment, livers and pancreas were fixed in formalin and mounted on slides for immunohistochemistry analysis.

Cell processing and isolation

Dissected orthotopic pancreatic tumors and murine livers with diffuse metastases were collected on Day 16 following tumor inoculation by the orthotopic and hemispleen procedure respectively, for analysis of tumor infiltrating lymphocytes (TILs). Each was mechanically processed sequentially through 40-μm and 100-μm nylon filters and brought to a volume of 20 mL of CTL medium. Suspensions were centrifuged at 1500 rpm for 5 minutes. Cell pellets were suspended in 4 mL of ACK lysis (Quality Biological) and subsequently spun at 1500 rpm for 5 minutes. Liver cell pellets were then resuspended in 6 mL 80% Percoll (GE Healthcare LifeSciences), overlaid with 6 mL 40% Percoll and

centrifuged at room temperature for 25 minutes at 3200 rpm without brake. The lymphocyte layer was removed and quenched with 30mL of CTL media.

Direct Technique isolation for fibroblast cells was performed using the Cellection Biotin Binder Kit (LifeTechnologies) and the sheep anti-human FAP biotinylated affinity purified antibody (R&D Systems Inc.) from processed tumor. Isolated TILs were enriched for $CD8^+$ cells using negative isolation kits (LifeTechnologies) and $CD11b^+$ cells using CD11b positive beads (LifeTechnologies) according to manufacturers' protocols.

Flow Cytometry

Processed cells from each mouse were stained with Live Dead Aqua Dead Cell Kit (Invitrogen) for 30 minutes on ice, washed with PBS and then blocked with rat anti-mouse Fc antibody (CD16/CD32 clone 2.4G2, BD Biosciences) in FACs buffer for 10 minutes. Following blocking, cells were stained for the following anti-mouse fluorophores for 1 hour on ice: CD3-PerCP Cy5.5 (Biolegend), CD3-APC Cy7 (Biolegend), CD4-APC Fire (Biolegend), CD8-PE Cy7 (Biolegend), CD44-PE (Biolegend), CD62L-APC (Biolegend), CCR7-BV421 (Biolegend), CD11b-PETR (ThermoFisher), Ly6C-PerCP Cy5.5 (Biolegend), Ly6G-V450 (Biolegend), F480-PE (ThermoFisher), and CXCR4-APC (Biolegend). Cells were then washed, resuspended in FACs buffer and assayed on a Cytoflex flow cytometer (Beckman Coulter). FACs buffer consisted of HBSS (Sigma) with 2% bovine calf serum (Sigma), 0.1% sodium azide (Sigma) and 0.1% HEPES.

The "total number" of immune cells was determined by the end gated count by FACS analysis of the single cell suspension and represent the absolute number of cells infiltrating in the entire analyzed tissue. The "percentage" of immune cells represents the percentage of an immune cell subtype gated among the gated live immune cell counts as determined by Live Dead Aqua and the plot of side scatter vs forward scatter.

Immunohistochemistry and RNA sequencing

Tumor tissues for human correlative immunohistochemistry (IHC) staining were obtained from specimens collected in patients who underwent surgery concurrently at our institution under the Institutional Review Board-approved protocol NA_00074221(47). Informed consent was obtained for all patients and studies were conducted in accordance with recognized ethical guidelines. These patients received one dose of GVAX two weeks prior to resection. Formalin-fixed paraffin-embedded (FFPE) tissue blocks were sectioned at 5μm thickness. IHC staining was performed using Dako Catalyzed Signal Amplification system as previously described(48). Antigen-retrieval and IHC staining were performed manually for CXCR4 with mouse anti-human-CXCR4 (12G5)(ThermoFisher). Slides were de-identified, scanned and individually analyzed using HALO Image Analysis Software (PerkinElmer). Peritumoral stroma, excluding epithelium, was circled and analyzed with the Positive Pixel Count algorithm to quantify stromal cell surface CXCR4 expression. Cell density was defined by the ratio of the positive pixels divided by the total specified stromal area. A count of >1.5 pixels/mm^2 was considered high expression of CXCR4.

FFPE tissue sections were stained for HA using the immune-adhesin HTI-601 with DAB used as the chromogen as described in Jadin et al (49). Two slides were stained for every

tissue sample. For each pair, one slide was pretreated with recombinant human hyaluronidase PH20 in PIPES buffer at pH 5.5 to digest HA as a negative control. The other slide was pretreated with PIPES buffer alone leaving HA intact. Stained slides were evaluated manually for accumulation of HA using the VMSI scoring algorithm (Halozyme, San Diego, CA). A VMSI score of ≥60 was considered high expression of HA.

FFPE tissue from the same human cohort of GVAX treated PDAC patients used for IHC had stroma microdissected, RNA purified and amplified as previously described(47). Whole exome RNA sequencing was performed at MedGenome, (Foster City, CA). In brief, cDNA was generated from the cleaved RNA fragments using random priming during first and second strand synthesis and sequencing adapters were ligated to the resulting double-stranded cDNA fragments. The coding regions of the transcriptome were then captured from this library using sequence-specific probes to create the final stranded RNA-Seq library. Reads mapping to ribosomal and mitochondrial genome were removed before performing alignment. Unwanted sequences, especially nonpolyA tailed RNAs, and contamination were removed. Paired-end reads were aligned to the reference human genome GRCh37/hg19. Raw read counts were normalized to the total prior to analysis, whereby the geometric mean was calculated for each gene across all samples. The counts for a gene in each sample were then divided by this mean. The data discussed in this publication have been deposited in the MINSEQE-compliant public NCBI's Gene Expression Omnibus(50) and are accessible through GEO Series accession number GSE125506. *CXCR4* expression of ≥4000 was considered high based upon the distribution of normalized *CXCR4* expression across all groups. Reference genes expression were calculated including *GAPDH* (median normalized read count=25,482) and *ACTB* (median normalized read count=174,687). Heat maps were generated using the Heatmapper software suite(51).

Statistical Analysis

Statistical analyses and graphing were performed using GraphPad Prism software (GraphPad Software, SanDiego, CA). Kaplan-Meier curves and log-rank tests were performed for survival estimates. One-way ANOVA or Student *t* tests were applied to compare the mean value among or between groups. A p-value of <0.05 was considered statistically significant.

Additional methods detail in supplemental files.

RESULTS

Untreated PDAC in murine liver and pancreas have high expression of HA that is effectively degraded by PEGPH20

To assess whether PEGPH20 effectively targeted HA in murine PDAC, we performed IHC of HA on resected liver and pancreas in our surgically implanted PDAC murine models. KPC tumor cells derived from the genetically engineered KPC mouse mirror human PDACs in their pathogenesis and immunobiology, including an inflammatory reaction and exclusion of effector T-cells, and as a result are as difficult as human PDACs to treat by immunotherapeutic agents(40). We found that in both our hemispleen model of liver metastases and our orthotopic pancreatic implantation model, that HA was highly expressed

and focally located in stromal islands surrounding the untreated tumor itself (Figure 1A, B). We then examined whether PEGPH20 could effectively target and degrade the HA in the stroma. To this end, IHC analysis of HA expression in tumor-bearing murine liver and pancreas was performed after mice were treated with one dose of PEGPH20(40μg/kg) and were sacrificed in series performing IHC of HA on murine liver and pancreas at different time intervals following drug administration. As shown in Figure 1, HA was effectively degraded in both liver and pancreas stroma following PEGPH20. This effect was transient as HA began to reappear at approximately one week and was again highly expressed in the tumor stroma at two weeks. This demonstrates that our murine model appropriately reflects the high HA stroma content in human PDAC, and that PEGPH20 effectively targets and transiently degrades this HA after one dose.

PEGPH20 enhances vaccine induced $CD4^+$ and $CD8^+$ T-cell infiltration into the tumor microenvironment

Next, we examined whether PEGPH20 could enhance the intratumoral infiltration of T-cells. As vaccine therapy, such as the GVAX vaccine, can induce tumor antigen specific T-cells(52), we examined whether PEGPH20 treatment can enhance T-cell infiltration into GVAX-treated tumors in two mouse models of PDAC. As described above, mice in these two models were either inoculated with KPC tumors orthotopically into the pancreas or spontaneous hepatic metastases were formed following an injection of KPC tumor cells through the hemisplenectomy procedure. Tumor-bearing mice were treated starting on Day 6 to allow tumor implantation and stromal development. On Day 16, dissected primary pancreatic tumors or livers with diffuse metastases were harvested, respectively, for fluorescence-activated cell sorting (FACS) analysis of TILs (Supplemental Figure 2). A significant increase in the total number of infiltrating $CD3^+CD8^+$ T-cells was observed with the PEGPH20/GVAX combination treatment comparing to untreated and single agent PEPGH20 or GVAX treated tumors in both the orthotopic and hemispleen mouse models (Figure 2A, B). Additionally, a significant increase in the relative percentage of infiltrating $CD3^+CD8^+$ T-cells was appreciated in the PEGPH20/GVAX combination treatment comparing to single agent GVAX treatment when analyzing the total TIL of dissected orthotopic tumors (Figure 2A). The relative percentage of $CD3^+CD8^+$ T-cells among total infiltrating immune cells was also significantly increased with the PEGPH20/GVAX combination treatment compared to untreated or PEPGH20 treatment when analyzing the TIL of metastatic tumors in the hemispleen model, with a positive trend compared to the GVAX treatment (Figure 2B). A significant increase in the relative percentage of infiltrating $CD3^+CD4^+$ T-cells was also observed in the TIL of dissected orthotopic tumors with the PEGPH20/GVAX combination treatment compared to single agent PEGPH20 or untreated controls, with a similar positive trend that did not reach statistical significance when compared to GVAX treatment (Figure 2C). Nevertheless, the relative percentage and absolute number of $CD3^+CD4^+$ T-cells was significantly increased with the PEGPH20/GVAX combination treatment compared to single agent or untreated controls in the analysis of the TIL of metastatic tumors (Figure 2D). There are slight discrepancies between the absolute number of tumor infiltrating $CD4^+$ and $CD8^+$ T-cells and the percentage of these $CD4^+$ and $CD8^+$ T-cells among the total immune infiltrates in the two different PDAC models. These discrepancies could be attributed to changes in the infiltration of other

immune cell subtypes, thus indirectly affecting the percentage of T-cells among the total immune infiltrates. Nevertheless, the results obtained from two different PDAC models are overall consistent. Of note, PEGPH20 as a single agent did not significantly enhance the percentage or absolute number of T-cells within the TME. We reasoned that the intratumoral infiltration of $CD8^+$ T-cells that are enhanced by PEGPH20 are predominantly not tumor antigen-specific. By contrast, the GVAX treatment is known to induce tumor-specific T-cells peripherally(52), and thus provides more tumor-specific T cells that can then traffic efficiently into the tumors as a result of the PEGPH20 treatment. These data from both murine PDAC models, suggest that stromal HA depletion by PEGPH20 may allow improved access and infiltration of T-cells within the TME potentially enhancing antitumor effects.

PEGPH20 in sequential combination with GVAX improves survival in a murine model of PDAC

We then tested whether targeted HA stromal depletion with PEGPH20 can augment the anti-tumor activity of immunotherapy when given in sequence with GVAX. We chose not to use the orthotopic model to perform efficacy experiments because we found that PEGPH20 treatment led to an immediate, transient decrease of the measured size of tumors presumably due to the depletion of stroma, thus inaccurately reflecting the actual tumor volumes. Therefore, the hemispleen model was utilized for efficacy experiments. The PEGPH20/GVAX combination treatment resulted in significantly improved survival of mice compared to GVAX or PEGPH20 as single agents (Figure 2E). No statistically significant difference was appreciated between the untreated and PEGPH20-treated mice. GVAX in combination with anti-PD1 antibody served as a positive control and similarly resulted in improved survival over GVAX as a single agent (Supplemental Figure 3A). However, combination treatment with PEGPH20, GVAX and anti-PD1 antibody did not offer additional survival benefit (Supplemental Figure 3B).

This may be explained by observations of the FACS analysis of dissected orthotopic tumors, whereby, expression of PD-L1 within the myeloid and macrophage subsets in pancreatic tumors was not induced in PEGPH20-treated mice as compared to untreated mice (Supplemental Figure 4A–B). By contrast, a trend towards an increased percentage of PD-L1 expression in the intratumoral myeloid cells was noted in mice that received GVAX treatment. Similarly, the relative expression of PD1 within the $CD3^+CD8^+$ T-cell subset in the pancreatic tumors was also not induced by PEGPH20 treatment (Supplemental Figure 4C). However, GVAX treatment induced a significant increase in the relative percentage of PD1 expression in $CD3^+CD8^+$ T-cells as compared to untreated mice. Interestingly, mice treated with the PEGPH20/GVAX combination, had lower PD1 expression comparing to GVAX-treated mice (Supplemental Figure 4C). The number of $PD1^+CD8^+$ cells has previously been predictive of sensitivity to checkpoint inhibitor therapy(7). Our results may explain why adding anti-PD1 antibody did not further improve the survival of the mice treated with the PEGPH20/GVAX combination (Supplemental Figure 3A). Thereby, these expression data are consistent with our survival experiments and suggest that PEGPH20 alone does not effectively prime the tumor microenvironment for effective anti-PD1 or anti-PD-L1 therapy.

To assess if the improved survival is T-cell dependent, $CD8^+$ T-cell depletion was performed starting on day 3 following the hemispleen procedure. No significant difference was appreciated between the untreated mice and $CD8^+$ depleted mice receiving the PEGPH20/GVAX combination treatment. A significant survival advantage was then appreciated when comparing the PEGPH20/GVAX combination treatment without $CD8^+$ depletion to the PEPGH20/GVAX combination treatment with $CD8^+$ depletion or compared to untreated mice. (Figure 2F). In summary, these data suggest that PEGPH20 enhances the immunologic anti-tumor effect of vaccine treatment, improving survival in a $CD8^+$ T-cell dependent manner in tumor bearing mice.

Targeting the stroma with PEGPH20 alters the CXCL12/CXCR4/CCR7 immunosuppressive signaling axis within the tumor microenvironment

Degradation of stromal HA by PEGPH20 reduces interstitial pressure, improves vascular perfusion and increases access of anticancer therapies in PDAC(17–20). We assessed if PEGPH20's targeted remodeling of tumor stroma may also affect the stroma's immunosuppressive signaling. Because myeloid cells are prevalent role players within the stroma, we first assessed if the number of myeloid cells ($CD3^-CD11b^+$) within the TME was altered by FACS. While a trend towards decreased myeloid cells was appreciated, a significant difference was not identified with PEGPH20 treatment or the PEGPH20/GVAX combination treatment in neither the orthotopic nor hemispleen models (Supplemental Figure 5). While significant quantitative differences were not noted, remodeling of the tumor stroma may affect qualitative function of these myeloid cells. Therefore, we used qPCR to analyze the mRNA gene expression of a large panel of T-cell trafficking related signals in the myeloid cells isolated from TIL with $CD11b^+$ beads. RNA was extracted and qPCR analysis revealed the majority of these, including chemokines such as *Cxcl9*, *Cxcl10*, *Cxcl11*, and *Ccl2*, are not significantly affected following PEGPH20 treatment (data not shown); however, a significant upregulation of *Cxcr4* expression in single agent GVAX treated groups was appreciated. This upregulation of *Cxcr4* expression after single agent GVAX treatment was significantly mitigated with the combination PEGPH20 and GVAX treatment in both the orthotopic (Figure 3A) and hemispleen models(Figure 3B). This change in expression was consistent with the identified changes of infiltrating T-cells on FACS, as CXCR4 signaling can inhibit T-cell accumulation. This suggests that the stromal remodeling by PEGPH20 decreases myeloid CXCR4 expression upregulated by GVAX, and may serve as an additional mechanism beyond decreased vascular impedance for enhanced T-cell infiltration. Immune analysis by flow cytometry supported these qPCR expression results. While the total number of myeloid cells was not decreased (Supplemental Figure 5), the PEGPH20/GVAX combination treatment diminishes the percentage of live $CD3^-CD11b^+$ cells that specifically expressed CXCR4 (Figure 3C).

The expression of CXCR4's ligand CXCL12 in FAP^+ CAFs has previously been shown to play a role in PDAC immune suppression (38). CAF cells were isolated from TIL with FAP^+ beads and RNA was extracted. Stromal depletion by PEGPH20 in the setting of GVAX decreases *Cxcl12* gene expression in CAF cells (Figure 3D). Notably, *Cxcl12* gene expression itself was not significantly affected by single agent treatment, including GVAX alone.

Because modulation of the CXCR4 signal in myeloid cells was associated with a change in T-cell infiltration and function, we therefore investigated the gene expression of *Ccr7*, a downstream signal of CXCR4, in $CD8^+$ cells. CXCR4 signaling is deemed important for stable *Ccr7* gene expression, facilitates CCR7 ligand binding and can affect trafficking function(53,54). For this study, $CD8^+$ cells were isolated from TIL by negative selection and RNA isolated. Similar to *Cxcr4* expression in myeloid cells, *Ccr7* was upregulated with single agent GVAX treatment and decreased with the PEGPH20/GVAX combination treatment (Figure 4A). These results provide an additional mechanistic explanation of why stromal remodeling by PEGPH20 enhances $CD8^+$ lymphocyte infiltration beyond increased therapeutic vascular perfusion in the setting of vaccine therapy.

Stromal signaling changes induced by PEGPH20 are associated with increased effector memory $CD8^+$ T-cell subtype percentage and number with improved antitumor activity

To determine if altered stromal signaling by PEGPH20 enhanced the quality of infiltrating $CD8^+$ T-cells, we assessed IFNγ production as well as the percent of naïve, effector and central memory T-cells by FACS. The above results suggest that the mechanism by which PEGPH20 enhanced vaccine-induced immune effect is by altering stromal signaling. One of the genes whose expression was decreased by the PEGPH20/GVAX combination treatment was *Ccr7*, a receptor found in $CD8^+$ T-cells associated by FACS surface markers with naïve T-cells ($CD8^+CD44^-CD62L^+CCR7^+$) and central memory T-cells ($CD8^+CD44^+CD62L^+CCR7^+$). Of note, effector memory T-cells ($CD8^+CD44^+CD62L^-CCR7^-$) do not express *Ccr7*(55). We thus performed FACS analysis of TIL from tumor-bearing mice to investigate if the proportion of infiltrating $CD8^+$ T-cell subtype was altered with combination treatment. Notably, treatment with GVAX as a single agent or in combination with PEGPH20, resulted in an increased absolute number of naïve T-cells within the TIL compared to untreated or PEPGH20 treated mice (Figure 4B). Interestingly, despite a greater total number, the PEGPH20/GVAX combination treatment resulted in a significantly lower relative percentage of total $CD8^+$ T-cells characterized as naïve by FACS surface markers (Figure 4B). Both the relative percentage and total number of $CD8^+$ T-cells with central memory markers were increased in mice treated with GVAX as single agent or in combination with PEGPH20 treatment (Figure 4C). Notably, while the total number and percentage of $CD8^+$ T-cells with effector memory markers were increased with single agent GVAX treatment, the PEGPH20/GVAX combination treatment resulted in an additional significant increase of the effector $CD8^+$ T-cell subset within the TIL (Figure 4D). These results suggest that the PEGPH20/GVAX combination treatment leads to enhanced infiltration of effector $CD8^+$ T-cells compared to untreated or single agent treated mice. In addition, following the PEGPH20/GVAX combination treatment, the effector phenotype makes up the greatest proportion of the total T-cells infiltrating the tumor.

Next, we assessed for tumor specific $CD8^+$ T-cell activity with murine IFNγ ELISA analysis by co-culturing irradiated autologous tumor cells to serve as a tumor-specific effector T-cell target. The PEGPH20/GVAX combination treatment significantly increased the tumor-specific IFNγ secretion by $CD8^+$ T-cells in the TME compared to single agent or untreated therapies (Figure 4E). Similarly, qPCR analysis of isolated $CD8^+$ T-cells from TIL revealed increased expression of *Ifnγ* (Figure 4F). Taken together, these data suggest that PEGPH20

modulates stromal CXCL12/CXCR4/CCR7 signaling in the presence of GVAX, resulting in increased infiltration of the effector $CD8^+$ subtype and increased tumor-specific IFNγ activity.

High HA expression in human PDAC tissue treated with GVAX is associated with the CXCR4 signaling axis and T-cell infiltration

IHC of HA and CXCR4 were performed on PDACs surgically resected from patients treated with GVAX two weeks prior to surgical resection (n=21). We next leveraged original data from a previously published study using multiplex IHC of various immune cell markers to assess patterns of immune cell infiltration in these human PDAC specimens(56). As the majority of PDACs express HA in the stroma, which may have more or less suppressed the $CD4^+$ and $CD8^+$ T-cell infiltration, HA status did not have significant associations with $CD8^+$ or $CD4^+$ T-cell infiltration (Supplemental Figure 6). However, as anticipated based on our findings in the mouse model, high HA expression was significantly associated with high CXCR4 expression within the stroma, and similarly low CXCR4 expression with lower HA (Figure 5A, B). Further investigation of the relationships of CXCR4 and immune cell infiltration was then performed. These data show that human PDAC tumor with low stromal CXCR4 expression have a higher percentage of $CD8^+$ cells infiltrating the tumor (Figure 5C). Furthermore, a significant increase in the proinflammatory IL17 expressing T-cells was also seen in PDAC tumor with low CXCR4 expression (Figure 5D). Changes were not appreciated in Th0, Th1 or Th2 cells (Figure 5E–G). Similarly, no significant difference was noted with the quantity of myeloid subsets of cells (Supplemental Figure 6). A heat map was generated to visualize the relationship of protein expression of CXCR4 and the density of immune cell infiltrates, particularly $CD8^+$ T-cells, according to the quantification of IHC results (Figure 5H). It demonstrated that low expression of CXCR4 correlates with increased intratumoral infiltration of $CD8^+$ T-cells and many other subtypes of T helper cells.

RNA sequencing data of dissected pancreatic specimen stroma was performed and high and low stromal *CXCR4* gene expression determined. Consistently, low *CXCR4* gene expression in PDAC stroma was correlated with high expression of cytotoxic effector T-cell activity including Granzyme A, IFNγ and Perforin (Figure 5 I–K). A second heat map was generated to visualize the relationship between the RNA expression of CXCR4 and the expression of markers of effector T-cell function including: *IFNα, IFNγ, IFNβ, GZMA* and *PRF1* (Figure 5L). It demonstrated that low RNA expression of *CXCR4* correlates with increased effector T-cell function.

Overall survival (OS) and progression free survival (PFS) outcomes of the patients with CXCR4 high and CXCR4 low tumors was also investigated. A trend towards shorter OS and PFS was noted in CXCR4 high tumors in patients who received GVAX treatment(47) (median OS: 11.5 months in CXCR4 high vs 35.3 months in CXCR4 low, p=0.24; median PFS: 9.6 months in CXCR4 high vs 31.4 months in CXCR4 low, p=0.59) although statistical significance was not met, likely due to small sample sizes (Supplemental Figure 7). Together these expression patterns show similar associations of the TME in human PDAC to our murine studies in regards to HA, stromal CXCR4 expression, downstream T-cell infiltration and effector function. This suggests CXCR4 remains a promising therapeutic target and the

potential downregulation of this pathway may also result in enhanced anti-tumor effect as seen with combination PEGPH20 and GVAX treatment in our preclinical murine model.

We further investigated PD-L1 expression in GVAX treated human PDAC tumor utilizing multiplex immunohistochemistry and the HA high and low subgroups. Low HA expression was not associated with any change in the percentage of PD-L1 expression in myeloid or macrophage cells. The relative expression of PD1 on $CD8^+$ cells was also not significantly increased in the HA low subgroup (Supplemental Figure 8A–C). An association with PD-L1 and PD-L2 gene expression with RNAseq was also investigated within the HA high vs HA low tumors. To this end, no significant difference was appreciated in the expression of *CD274* (PD-L1) nor *PDCD1LG2* (PD-L2) when comparing the HA high and HA low subgroups (Supplemental Figure 8D, E). This is consistent with the findings in our mouse model that the targeted degradation of HA by PEGPH20 does not induce significant PD1 or PD-L1 expression thus failing to effectively prime for anti-PD1 or anti-PD-L1 therapy.

DISCUSSION

Presented here is the first study in PDAC of a stromal targeting agent that modulates the myeloid cells thereby increasing the effector memory T-cell subset within the tumors. Despite rapid progress for immunotherapy in multiple cancer biologies, PDAC remains largely resistant with dismal patient survival. The optimal treatment regimen for PDAC will likely require rational combinations of therapeutics in order to improve patient prognoses(43). An effective stromal-targeting agent is imperative for the immunotherapy armamentarium in order to overcome desmoplasia, manipulate the microenvironment's signaling cascade, and allow for optimal drug delivery and immune surveillance. In this report, we find that targeted HA depletion with PEGPH20 in combination with the irradiated whole cell PDAC vaccine GVAX, decreases expression of the CXCL12/CXCR4/CCR7 immunosuppressive signaling axis in CAFs, myeloid and $CD8^+$ cells respectively. This corresponded with an increase in infiltration of the CCR7(−) effector memory T-cell subset in the combination treatment group with associated increase in tumor specific IFNγ and improved mouse survival compared to single agent therapies. These findings suggest that remodeling the PDAC peritumoral stroma via HA depletion with PEGPH20 can modify the function of myeloid cells leading to downstream increases in $CD8^+$ T-cell infiltration and anti-tumor function in the setting of GVAX. In human PDAC tissue, low CXCR4 expression in dissected stroma consistently correlated with high expression of markers of cytotoxic effector T-cell activity such as *PRF1*, *IFNγ* and *GZMA*, supporting CXCR4 as a promising target for PDAC therapy. Furthermore, initial patterns associating low HA expression, low CXCR4 expression and high $CD8^+$ T-cell infiltration in these GVAX treated human PDAC specimens suggests manipulation of this pathway by PEGPH20 may also enhance anti-tumor effector function, and thus this preclinical study may have future translatability in human patients.

We hypothesize that HA within the TME activates resident CAFs to produce more CXCL12 and subsequently activate CXCR4. HA depletion and stromal modulation with PEGPH20 treatment then interferes with this pathway abrogating these downstream effects (Figure 6). Thus, one would anticipate decreased *Cxcl12* gene expression in CAF cells following single

agent PEGPH20 treatment, although this was not observed in this study. However, it was decreased in tumor treated with both PEGPH20 and GVAX. It remains to be investigated why the effect of PEGPH20 on the expression of *Cxcl12* from CAF is associated with GVAX treatment. The upregulated immunosuppressive pathway within the stroma in response to GVAX treatment may diminish maximal therapeutic effect of the vaccine and offer insight to why the vaccine has been ineffective as a single agent for PDAC(57). PEGPH20 serves to mitigate these upregulated signals on CXCR4 pathway in the presence of GVAX treatment synergizing and enhancing its anti-tumor immunologic effects.

In this study, we see that treatment with single agent GVAX upregulates myeloid *Cxcr4* expression and subsequently $CD8^+$ cell *Ccr7* expression in parallel. The addition of PEGPH20 modulates these cells mitigating the upregulation and resulting in significantly decreased *Cxcr4* expression. In accordance, *Ccr7* expression was also downregulated following the PEGPH20/GVAX combination treatment. This further supports the relationship of CXCR4 and CCR7 within the signaling cascade and the proposed potential benefit of targeted inhibition of this pathway. Interestingly while overall *Ccr7* expression was decreased and the infiltration of CCR7(−) effector memory T-cells enhanced, no significant difference in the total number of infiltrating $CCR7^+$ central memory cells was observed in the combination treatment group compared to single agent therapies. Manipulation of the TME to enhance effector memory T-cells is imperative as a naturally occurring tumor-reactive T-cell response in untreated PDAC is limited in quantity and quality(8).

While the lengthened survival in mice treated with combination treatment is encouraging, no mice were cured in this study. However, when compared to other studies utilizing the hemispleen model, treatment was notably delayed following tumor implantation in an attempt to ensure PEGPH20's treatment was acting on the desmoplastic peritumoral stroma as opposed to preventing tumor establishment(43). This delay resulted in a more aggressive tumor biology and earlier murine death. Additionally, only a single dose of vaccine was given for this study which has previously been shown not to cure mice(43). Multiple cycles were not used in this study due to the initial observance of disrupted postoperative wound healing and flank tumors following repetitive treatments in these mice shortly following their procedure.

GVAX treatment permits T-cell infiltration into the PDAC tumor not previously seen in the untreated immune excluded tumors(43,47). GVAX treatment however leads to a parallel increase of immunosuppressive and exhausted signals: more PD1 expression, more MDSC and tumor associated macrophage infiltration, and upregulation of pathways such as myeloid CXCR4. This provided the rationale for the use of previously ineffective checkpoint blockade in combination with GVAX. However, preliminary data did not show synergistic effects with the addition of anti-PD1 antibody to PEGPH20 and GVAX in a triple combination (Supplementary Figure 3A). In this study, PEGPH20 influences the phenotype of T-cells that infiltrate the tumor by decreasing *Ccr7* expression thereby enhancing the CCR7(−) effector subtype in the setting of GVAX treatment. While anti-PD1 antibody interrupts the checkpoint cascade broadly improving T-cell exhaustion, it is possible it has a less optimal role in this "preselected" phenotype of effector cells, thereby explaining a lack

of synergy. In the future, further consideration combining PEGPH20 with T-cell agonists instead of GVAX may be prudent and remains to be explored.

The human PDAC tissue for this study was subgrouped by HA expression. In the future, it will be intriguing to examine the effect of targeted HA depletion on the myeloid cells and effector memory T-cells in pancreatic specimen from a clinical trial investigating treatment with PEGPH20. Additional investigation focusing more on the signaling of CXCR4 is also of interest. Associations of low HA, low CXCR4 and high $CD8^+$ and TH17 infiltration suggest a similar effect may be seen with combination PEGPH20 treatment in human PDAC. The density of myeloid cells was not distinctly different in HA high vs HA low groups amongst GVAX treated human PDAC (Supplemental Figure 6) suggesting that the quantity of the myeloid cells is unlikely to be affected by PEGPH20 treatment. Consistently in our animal model, PEGPH20 treatment correlates with decreased *Cxcr4* stromal cell expression, but does not significantly influence total myeloid cell number. Therefore, our study suggests that the $CXCR4^+$ myeloid cells are the targets of stromal modulating immunotherapy.

The findings of this study are limited to the setting of GVAX treatment. PDAC is known to be an immune desert with scarce T-cells at baseline, and thus it is necessary to use a T-cell priming agent in combination with stroma targeting agents to assess the latter's immune modulating effects of stroma targeting agents PEPGH20 treatment alone may increase $CD8^+$ T-cell infiltration, however, a survival advantage of single agent treatment was not appreciated in this study, perhaps due to a lack of tumor antigen-specific cells. Conversely, GVAX treatment induces tumor antigen-specific effector T-cells within the periphery(43,47), that may then more effectively infiltrate the TME when used in combination with PEGPH20 treatment. Future studies will need to examine whether PEGPH20 has a similar or different immune modulating effects with alternative T-cell priming agents. As we did not observe synergistic effect of the combination of PEGPH20 and anti-PD1 antibodies, it remains to be explored what other immune modulating agents can synergize with the myeloid modulating effect of PEGPH20. For example, inhibitors of Focal Adhesion Kinase (FAK) have shown encouraging effects in preclinical models of PDAC with an ability to modulate the myeloid compartment by targeting stromal signaling(58). It would be intriguing to examine whether the simultaneous targeting of extracellular stromal signaling with PEGPH20 and intracellular stromal signaling with FAK inhibitor would have a synergistic effect on myeloid cell modulation.

Supplementary Material

Refer to Web version on PubMed Central for supplementary material.

ACKNOWLEDGEMENTS

We acknowledge and thank MedGenome for cost sharing of RNA sequencing efforts.

Financial support: This work was supported in part by a grant from Halozyme; NIH grant T32 CA126607 (ABB and LZ); NIH grant R01 CA169702 (LZ); NIH grant K23 CA148964(LZ); NIH grant R01 CA197296(LZ); the Viragh Foundation and the Skip Viragh Pancreatic Cancer Center at Johns Hopkins (EMJ and LZ); the Sol Goldman Pancreatic Cancer Research Center (LZ); the Lefkofsky Family Foundation (LZ); National Cancer

Institute Specialized Programs of Research Excellence in Gastrointestinal Cancers grant P50 CA062924 (EMJ and LZ); Sidney Kimmel Comprehensive Cancer Center grant P30 CA006973 (EMJ and LZ); and a Lustgarten Foundation grant (LZ).

References:

1. Pardoll D. Cancer and the Immune System: Basic Concepts and Targets for Intervention. Semin Oncol 2015;42(4):523–38 doi 10.1053/j.seminoncol.2015.05.003. [PubMed: 26320058]
2. Topalian SL, Hodi FS, Brahmer JR, Gettinger SN, Smith DC, McDermott DF, et al. Safety, activity, and immune correlates of anti-PD-1 antibody in cancer. N Engl J Med 2012;366(26):2443–54 doi 10.1056/NEJMoa1200690. [PubMed: 22658127]
3. Wolchok JD, Kluger H, Callahan MK, Postow MA, Rizvi NA, Lesokhin AM, et al. Nivolumab plus ipilimumab in advanced melanoma. N Engl J Med 2013;369(2):122–33 doi 10.1056/NEJMoa1302369. [PubMed: 23724867]
4. Brahmer JR, Tykodi SS, Chow LQ, Hwu WJ, Topalian SL, Hwu P, et al. Safety and activity of anti-PD-L1 antibody in patients with advanced cancer. N Engl J Med 2012;366(26):2455–65 doi 10.1056/NEJMoa1200694. [PubMed: 22658128]
5. Royal RE, Levy C, Turner K, Mathur A, Hughes M, Kammula US, et al. Phase 2 trial of single agent Ipilimumab (anti-CTLA-4) for locally advanced or metastatic pancreatic adenocarcinoma. J Immunother 2010;33(8):828–33 doi 10.1097/CJI.0b013e3181eec14c. [PubMed: 20842054]
6. Fukunaga A, Miyamoto M, Cho Y, Murakami S, Kawarada Y, Oshikiri T, et al. CD8+ tumor-infiltrating lymphocytes together with CD4+ tumor-infiltrating lymphocytes and dendritic cells improve the prognosis of patients with pancreatic adenocarcinoma. Pancreas 2004;28(1):e26–31. [PubMed: 14707745]
7. Li J, Byrne KT, Yan F, Yamazoe T, Chen Z, Baslan T, et al. Tumor Cell-Intrinsic Factors Underlie Heterogeneity of Immune Cell Infiltration and Response to Immunotherapy. Immunity 2018;49(1):178–93 e7 doi 10.1016/j.immuni.2018.06.006. [PubMed: 29958801]
8. Stromnes IM, Hulbert A, Pierce RH, Greenberg PD, Hingorani SR. T-cell Localization, Activation, and Clonal Expansion in Human Pancreatic Ductal Adenocarcinoma. Cancer Immunol Res 2017;5(11):978–91 doi 10.1158/2326-6066.CIR-16-0322. [PubMed: 29066497]
9. Rucki AA, Zheng L. Pancreatic cancer stroma: understanding biology leads to new therapeutic strategies. World J Gastroenterol 2014;20(9):2237–46 doi 10.3748/wjg.v20.i9.2237. [PubMed: 24605023]
10. Rucki AA, Foley K, Zhang P, Xiao Q, Kleponis J, Wu AA, et al. Heterogeneous Stromal Signaling within the Tumor Microenvironment Controls the Metastasis of Pancreatic Cancer. Cancer Res 2017;77(1):41–52 doi 10.1158/0008-5472.CAN-16-1383. [PubMed: 27821486]
11. Multhaupt HA, Leitinger B, Gullberg D, Couchman JR. Extracellular matrix component signaling in cancer. Adv Drug Deliv Rev 2016;97:28–40 doi 10.1016/j.addr.2015.10.013. [PubMed: 26519775]
12. Ozdemir BC, Pentcheva-Hoang T, Carstens JL, Zheng X, Wu CC, Simpson TR, et al. Depletion of carcinoma-associated fibroblasts and fibrosis induces immunosuppression and accelerates pancreas cancer with reduced survival. Cancer Cell 2014;25(6):719–34 doi 10.1016/j.ccr.2014.04.005. [PubMed: 24856586]
13. Rhim AD, Oberstein PE, Thomas DH, Mirek ET, Palermo CF, Sastra SA, et al. Stromal elements act to restrain, rather than support, pancreatic ductal adenocarcinoma. Cancer Cell 2014;25(6):735–47 doi 10.1016/j.ccr.2014.04.021. [PubMed: 24856585]
14. Rogers HJ. The structure and function of hyaluronate. Biochem Soc Symp 1961;20:51–79. [PubMed: 13742759]
15. Sironen RK, Tammi M, Tammi R, Auvinen PK, Anttila M, Kosma VM. Hyaluronan in human malignancies. Exp Cell Res 2011;317(4):383–91 doi 10.1016/j.yexcr.2010.11.017. [PubMed: 21134368]
16. Whatcott CJ, Diep CH, Jiang P, Watanabe A, LoBello J, Sima C, et al. Desmoplasia in Primary Tumors and Metastatic Lesions of Pancreatic Cancer. Clin Cancer Res 2015;21(15):3561–8 doi 10.1158/1078-0432.CCR-14-1051. [PubMed: 25695692]

17. Jacobetz MA, Chan DS, Neesse A, Bapiro TE, Cook N, Frese KK, et al. Hyaluronan impairs vascular function and drug delivery in a mouse model of pancreatic cancer. Gut 2013;62(1):112–20 doi 10.1136/gutjnl-2012-302529. [PubMed: 22466618]

18. Li X, Shepard HM, Cowell JA, Zhao C, Osgood RJ, Rosengren S, et al. Parallel Accumulation of Tumor Hyaluronan, Collagen, and Other Drivers of Tumor Progression. Clin Cancer Res 2018 doi 10.1158/1078-0432.CCR-17-3284.

19. Provenzano PP, Cuevas C, Chang AE, Goel VK, Von Hoff DD, Hingorani SR. Enzymatic targeting of the stroma ablates physical barriers to treatment of pancreatic ductal adenocarcinoma. Cancer Cell 2012;21(3):418–29 doi 10.1016/j.ccr.2012.01.007. [PubMed: 22439937]

20. Thompson CB, Shepard HM, O'Connor PM, Kadhim S, Jiang P, Osgood RJ, et al. Enzymatic depletion of tumor hyaluronan induces antitumor responses in preclinical animal models. Mol Cancer Ther 2010;9(11):3052–64 doi 10.1158/1535-7163.MCT-10-0470. [PubMed: 20978165]

21. Brekken C, de Lange Davies C. Hyaluronidase reduces the interstitial fluid pressure in solid tumours in a non-linear concentration-dependent manner. Cancer Lett 1998;131(1):65–70. [PubMed: 9839621]

22. Jiang P, Li X, Thompson CB, Huang Z, Araiza F, Osgood R, et al. Effective targeting of the tumor microenvironment for cancer therapy. Anticancer Res 2012;32(4):1203–12. [PubMed: 22493350]

23. Manuel ER, Chen J, D'Apuzzo M, Lampa MG, Kaltcheva TI, Thompson CB, et al. Salmonella-Based Therapy Targeting Indoleamine 2,3-Dioxygenase Coupled with Enzymatic Depletion of Tumor Hyaluronan Induces Complete Regression of Aggressive Pancreatic Tumors. Cancer Immunol Res 2015;3(9):1096–107 doi 10.1158/2326-6066.CIR-14-0214. [PubMed: 26134178]

24. Elahi-Gedwillo KY, Carlson M, Zettervall J, Provenzano PP. Antifibrotic Therapy Disrupts Stromal Barriers and Modulates the Immune Landscape in Pancreatic Ductal Adenocarcinoma. Cancer Res 2019;79(2):372–86 doi 10.1158/0008-5472.CAN-18-1334. [PubMed: 30401713]

25. Hingorani SR, Zheng L, Bullock AJ, Seery TE, Harris WP, Sigal DS, et al. HALO 202: Randomized Phase II Study of PEGPH20 Plus Nab-Paclitaxel/Gemcitabine Versus Nab-Paclitaxel/Gemcitabine in Patients With Untreated, Metastatic Pancreatic Ductal Adenocarcinoma. J Clin Oncol 2018;36(4):359–66 doi 10.1200/JCO.2017.74.9564. [PubMed: 29232172]

26. Infante JR, Korn RL, Rosen LS, LoRusso P, Dychter SS, Zhu J, et al. Phase 1 trials of PEGylated recombinant human hyaluronidase PH20 in patients with advanced solid tumours. Br J Cancer 2018;118(2):e3 doi 10.1038/bjc.2017.438.

27. Ramanathan RK, McDonough SL, Philip PA, Hingorani SR, Lacy J, Kortmansky JS, et al. Phase IB/II Randomized Study of FOLFIRINOX Plus Pegylated Recombinant Human Hyaluronidase Versus FOLFIRINOX Alone in Patients With Metastatic Pancreatic Adenocarcinoma: SWOG S1313. J Clin Oncol 2019:10.1200/JCO.18.01295.

28. Singha NC, Nekoroski T, Zhao C, Symons R, Jiang P, Frost GI, et al. Tumor-associated hyaluronan limits efficacy of monoclonal antibody therapy. Mol Cancer Ther 2015;14(2):523–32 doi 10.1158/1535-7163.MCT-14-0580. [PubMed: 25512619]

29. Zheng L, Xue J, Jaffee EM, Habtezion A. Role of immune cells and immune-based therapies in pancreatitis and pancreatic ductal adenocarcinoma. Gastroenterology 2013;144(6):1230–40 doi 10.1053/j.gastro.2012.12.042. [PubMed: 23622132]

30. Gabrilovich DI, Ostrand-Rosenberg S, Bronte V. Coordinated regulation of myeloid cells by tumours. Nat Rev Immunol 2012;12(4):253–68 doi 10.1038/nri3175. [PubMed: 22437938]

31. Pergamo M, Miller G. Myeloid-derived suppressor cells and their role in pancreatic cancer. Cancer Gene Ther 2017;24(3):100–5 doi 10.1038/cgt.2016.65. [PubMed: 27910857]

32. Steele CW, Karim SA, Leach JDG, Bailey P, Upstill-Goddard R, Rishi L, et al. CXCR2 Inhibition Profoundly Suppresses Metastases and Augments Immunotherapy in Pancreatic Ductal Adenocarcinoma. Cancer Cell 2016;29(6):832–45 doi 10.1016/j.ccell.2016.04.014. [PubMed: 27265504]

33. Balkwill F. Cancer and the chemokine network. Nat Rev Cancer 2004;4(7):540–50 doi 10.1038/nrc1388. [PubMed: 15229479]

34. Caruz A, Samsom M, Alonso JM, Alcami J, Baleux F, Virelizier JL, et al. Genomic organization and promoter characterization of human CXCR4 gene. FEBS Lett 1998;426(2):271–8. [PubMed: 9599023]

35. Chen Y, Huang Y, Reiberger T, Duyverman AM, Huang P, Samuel R, et al. Differential effects of sorafenib on liver versus tumor fibrosis mediated by stromal-derived factor 1 alpha/C-X-C receptor type 4 axis and myeloid differentiation antigen-positive myeloid cell infiltration in mice. Hepatology 2014;59(4):1435–47 doi 10.1002/hep.26790. [PubMed: 24242874]

36. Duda DG, Kozin SV, Kirkpatrick ND, Xu L, Fukumura D, Jain RK. CXCL12 (SDF1alpha)-CXCR4/CXCR7 pathway inhibition: an emerging sensitizer for anticancer therapies? Clin Cancer Res 2011;17(8):2074–80 doi 10.1158/1078-0432.CCR-10-2636. [PubMed: 21349998]

37. Chen Y, Ramjiawan RR, Reiberger T, Ng MR, Hato T, Huang Y, et al. CXCR4 inhibition in tumor microenvironment facilitates anti-programmed death receptor-1 immunotherapy in sorafenib-treated hepatocellular carcinoma in mice. Hepatology 2015;61(5):1591–602 doi 10.1002/hep.27665. [PubMed: 25529917]

38. Feig C, Jones JO, Kraman M, Wells RJ, Deonarine A, Chan DS, et al. Targeting CXCL12 from FAP-expressing carcinoma-associated fibroblasts synergizes with anti-PD-L1 immunotherapy in pancreatic cancer. Proc Natl Acad Sci U S A 2013;110(50):20212–7 doi 10.1073/pnas.1320318110. [PubMed: 24277834]

39. Kraman M, Bambrough PJ, Arnold JN, Roberts EW, Magiera L, Jones JO, et al. Suppression of antitumor immunity by stromal cells expressing fibroblast activation protein-alpha. Science 2010;330(6005):827–30 doi 10.1126/science.1195300. [PubMed: 21051638]

40. Hingorani SR, Wang L, Multani AS, Combs C, Deramaudt TB, Hruban RH, et al. Trp53R172H and KrasG12D cooperate to promote chromosomal instability and widely metastatic pancreatic ductal adenocarcinoma in mice. Cancer Cell 2005;7(5):469–83 doi 10.1016/j.ccr.2005.04.023. [PubMed: 15894267]

41. Foley K, Rucki AA, Xiao Q, Zhou D, Leubner A, Mo G, et al. Semaphorin 3D autocrine signaling mediates the metastatic role of annexin A2 in pancreatic cancer. Sci Signal 2015;8(388):ra77 doi 10.1126/scisignal.aaa5823. [PubMed: 26243191]

42. Soares KC, Foley K, Olino K, Leubner A, Mayo SC, Jain A, et al. A preclinical murine model of hepatic metastases. J Vis Exp 2014(91):51677 doi 10.3791/51677. [PubMed: 25285458]

43. Soares KC, Rucki AA, Wu AA, Olino K, Xiao Q, Chai Y, et al. PD-1/PD-L1 blockade together with vaccine therapy facilitates effector T-cell infiltration into pancreatic tumors. J Immunother 2015;38(1):1–11 doi 10.1097/CJI.0000000000000062. [PubMed: 25415283]

44. Laheru D, Lutz E, Burke J, Biedrzycki B, Solt S, Onners B, et al. Allogeneic granulocyte macrophage colony-stimulating factor-secreting tumor immunotherapy alone or in sequence with cyclophosphamide for metastatic pancreatic cancer: a pilot study of safety, feasibility, and immune activation. Clin Cancer Res 2008;14(5):1455–63 doi 10.1158/1078-0432.CCR-07-0371. [PubMed: 18316569]

45. Machiels JP, Reilly RT, Emens LA, Ercolini AM, Lei RY, Weintraub D, et al. Cyclophosphamide, doxorubicin, and paclitaxel enhance the antitumor immune response of granulocyte/macrophage-colony stimulating factor-secreting whole-cell vaccines in HER-2/neu tolerized mice. Cancer Res 2001;61(9):3689–97. [PubMed: 11325840]

46. Leao IC, Ganesan P, Armstrong TD, Jaffee EM. Effective depletion of regulatory T cells allows the recruitment of mesothelin-specific CD8 T cells to the antitumor immune response against a mesothelin-expressing mouse pancreatic adenocarcinoma. Clin Transl Sci 2008;1(3):228–39 doi 10.1111/j.1752-8062.2008.00070.x. [PubMed: 20357913]

47. Lutz ER, Wu AA, Bigelow E, Sharma R, Mo G, Soares K, et al. Immunotherapy converts nonimmunogenic pancreatic tumors into immunogenic foci of immune regulation. Cancer Immunol Res 2014;2(7):616–31 doi 10.1158/2326-6066.CIR-14-0027. [PubMed: 24942756]

48. Bigelow E, Bever KM, Xu H, Yager A, Wu A, Taube J, et al. Immunohistochemical staining of B7-H1 (PD-L1) on paraffin-embedded slides of pancreatic adenocarcinoma tissue. J Vis Exp 2013(71) doi 10.3791/4059.

49. Jadin L, Huang L, Wei G, Zhao Q, Gelb AB, Frost GI, et al. Characterization of a novel recombinant hyaluronan binding protein for tissue hyaluronan detection. J Histochem Cytochem 2014;62(9):672–83 doi 10.1369/0022155414540176. [PubMed: 24891594]

50. Edgar R, Domrachev M, Lash AE. Gene Expression Omnibus: NCBI gene expression and hybridization array data repository. Nucleic Acids Res 2002;30(1):207–10. [PubMed: 11752295]

51. Babicki S, Arndt D, Marcu A, Liang Y, Grant JR, Maciejewski A, et al. Heatmapper: web-enabled heat mapping for all. Nucleic Acids Res 2016;44(W1):W147–53 doi 10.1093/nar/gkw419. [PubMed: 27190236]
52. Lutz E, Yeo CJ, Lillemoe KD, Biedrzycki B, Kobrin B, Herman J, et al. A lethally irradiated allogeneic granulocyte-macrophage colony stimulating factor-secreting tumor vaccine for pancreatic adenocarcinoma. A Phase II trial of safety, efficacy, and immune activation. Ann Surg 2011;253(2):328–35 doi 10.1097/SLA.0b013e3181fd271c. [PubMed: 21217520]
53. Kobayashi D, Endo M, Ochi H, Hojo H, Miyasaka M, Hayasaka H. Regulation of CCR7-dependent cell migration through CCR7 homodimer formation. Sci Rep 2017;7(1):8536 doi 10.1038/s41598-017-09113-4. [PubMed: 28819198]
54. Bai Z, Hayasaka H, Kobayashi M, Li W, Guo Z, Jang MH, et al. CXC chemokine ligand 12 promotes CCR7-dependent naive T cell trafficking to lymph nodes and Peyer's patches. J Immunol 2009;182(3):1287–95. [PubMed: 19155474]
55. Sallusto F, Geginat J, Lanzavecchia A. Central memory and effector memory T cell subsets: function, generation, and maintenance. Annu Rev Immunol 2004;22:745–63 doi 10.1146/annurev.immunol.22.012703.104702. [PubMed: 15032595]
56. Tsujikawa T, Kumar S, Borkar RN, Azimi V, Thibault G, Chang YH, et al. Quantitative Multiplex Immunohistochemistry Reveals Myeloid-Inflamed Tumor-Immune Complexity Associated with Poor Prognosis. Cell Rep 2017;19(1):203–17 doi 10.1016/j.celrep.2017.03.037. [PubMed: 28380359]
57. Le DT, Wang-Gillam A, Picozzi V, Greten TF, Crocenzi T, Springett G, et al. Safety and survival with GVAX pancreas prime and Listeria Monocytogenes-expressing mesothelin (CRS-207) boost vaccines for metastatic pancreatic cancer. J Clin Oncol 2015;33(12):1325–33 doi 10.1200/JCO.2014.57.4244. [PubMed: 25584002]
58. Jiang H, Hegde S, Knolhoff BL, Zhu Y, Herndon JM, Meyer MA, et al. Targeting focal adhesion kinase renders pancreatic cancers responsive to checkpoint immunotherapy. Nat Med 2016;22(8):851–60 doi 10.1038/nm.4123. [PubMed: 27376576]

Translational Relevance:

Pancreatic ductal adenocarcinoma (PDAC) has a dismal prognosis with broad resistance to therapeutics, due in part to its dense desmoplastic stroma. It has been long hypothesized that the stroma serves as both a physical barrier and a source of immunosuppressive signals. An effective stromal targeting agent able to overcome desmoplasia would be anticipated to permit immune surveillance. However, the role of stromal depletion in PDAC is controversial. Thus, in this study, we investigate the role of modulating the PDAC stroma and its signaling via the use of PEGylated human hyaluronidase (PEGPH20). For the first time, our study shows that targeting stroma in combination with vaccine therapy remodels the immunosuppressive signaling axis and subsequently enhances the effector memory T-cell infiltration in the tumors. This study thus suggests that PEGPH20 in combination with immunotherapy have a potential translatability in treating PDAC patients by enhancing immune anti-tumor effector memory T-cell function.

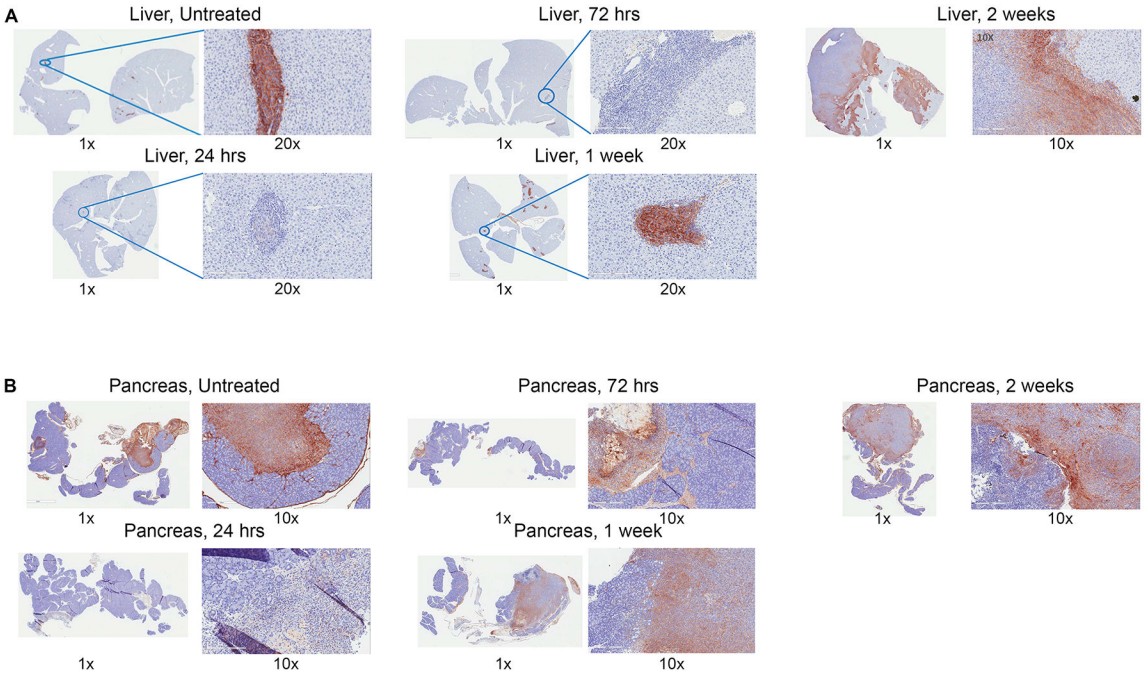

Figure 1. Hyaluronan is expressed in peritumoral stroma and is degraded by PEGPH20 in murine liver and pancreas.

Pancreatic adenocarcinoma was established by either the hemispleen procedure or orthotopic implantation. One dose of IV PEGPH20 (40μg/kg) was given to mice on Day 6 following surgery. Mice were sacrificed at periodic intervals following the single PEGPH20 treatment with corresponding liver and pancreas sectioned and embedded in FFPE. Untreated mice were sacrificed on Day 5. Immunohistochemistry for hyaluronan was performed in FFPE sections in (**A**) livers of hemispleen model mice (n=9) and (**B**) pancreata of orthotopic implantation model mice (n=9).

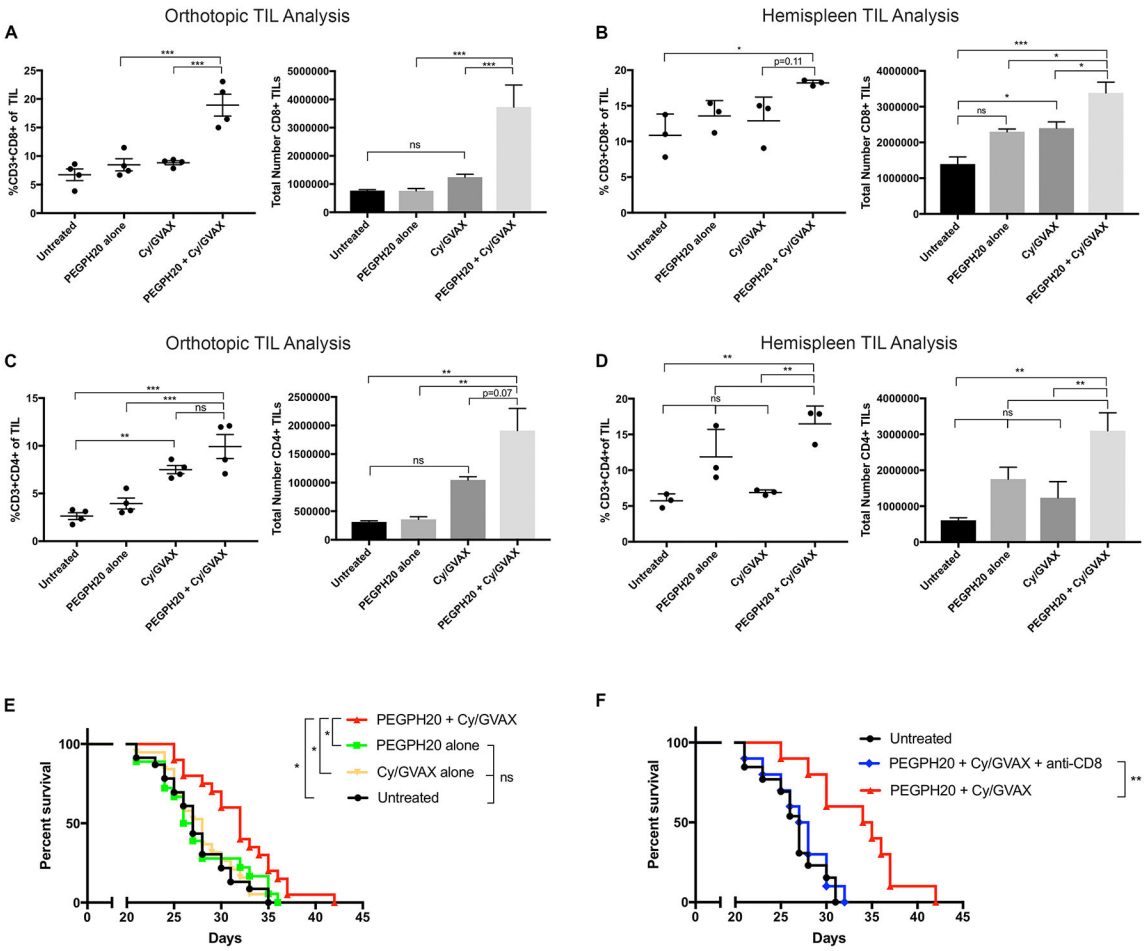

Figure 2. Tumor stromal depletion of hyaluronan by PEGPH20 in combination with GVAX enhances CD8$^+$ T-cell infiltration in PDAC and improves survival compared to single agent therapies.

Following the inoculation of KPC tumor cells by either orthotopic implantation or the hemispleen procedure, mice were treated with Cy (100 mg/kg) on Day 6, PEGPH20 (40μg/kg) on Day 6 and GVAX on Day 7. Flow cytometry was performed on tumor infiltrating lymphocytes (TIL) isolated from processed dissected orthotopic tumor or diffusely metastatic liver respectively. Each experimental group consisted of 3 or 4 mice analyzed individually. Relative percentage and total number of live CD3$^+$CD8$^+$ TIL in the combination PEPGH20/GVAX treatment group compared to single agent treatment groups in the (**A**) orthotopic model and (**B**) hemispleen model respectively. Relative percentage and total number of live CD3$^+$CD4$^+$ TIL in the combination PEGPH20/GVAX treatment group compared to single agent treatment groups in the (**C**) orthotopic model and (**D**) hemispleen model respectively. Data represent mean ± SEM from one representative experiment that was repeated three times. *ns* not significant, * p<0.05,** p<0.01, ***p<0.001. (**E**) Kaplan Meier survival curves of mice implanted with PDAC cells in untreated mice (n=22), mice treated with Cy/GVAX alone (n=18), PEGPH20 alone (n=18), or the combination PEGPH20/GVAX treatment (n=18). Data represent the combined data of two consecutive experiments. *ns* not significant, * p<0.05. (**F**) Kaplan Meier survival curves of mice

implanted with PDAC cells in untreated mice (n=10) or mice treated with the combination PEGPH20/GVAX treatment with $CD8^+$ T-cell depletion (n=10) and without $CD8^+$ T-cell depletion (n=10). *ns* not significant,** $p<0.01$.

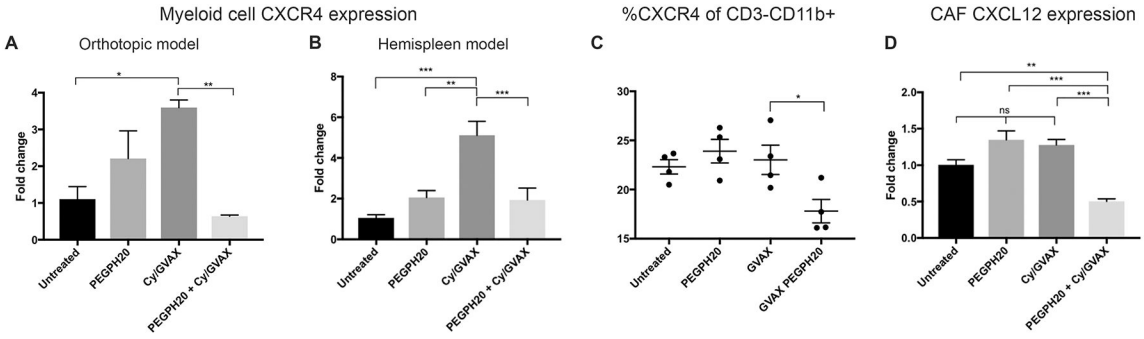

Figure 3. PEGPH20 in combination with GVAX decreases RNA expression within the CXCL12/CXCR4 signaling axis of cells in the tumor microenvironment.

Following the inoculation of KPC tumor cells by either orthotopic implantation or the hemispleen procedure, tumor-bearing mice were treated with Cy (100 mg/kg) on Day 6, PEGPH20 (40μg/kg) on Day 6 and GVAX on Day 7. Mice were sacrificed on Day 16. RNA was extracted from myeloid cells isolated with $CD11b^+$ beads from the tumor microenvironment of (**A**) dissected orthotopic tumors or (**B**) diffusely metastatic livers of hemispleen mice, respectively. Quantitative real-time reverse transcription polymerase chain reaction (qPCR) reveals patterns of myeloid *Cxcr4* expression in single agent treatments or the combination PEGPH20/GVAX treatment group (n=3 mice). (**C**) Flow cytometry was performed on tumor infiltrating lymphocytes (TIL) isolated from processed diffusely metastatic murine livers of hemispleen mice. Relative percentage of $CD3^-CD11b^+$ cells expressing CXCR4 as determined by immune analysis of 4 mice analyzed individually by flow cytometry. RNA was extracted from cancer associated fibroblasts isolated with FAP^+ beads from diffusely metastatic murine livers (n=3 mice). qPCR reveals patterns of CAF (**C**) *Cxcl12* expression (n=3 mice). Data represent mean ± SEM from one representative experiment that was repeated twice. *ns* not significant, * $p<0.05$,** $p<0.01$, ***$p<0.001$.

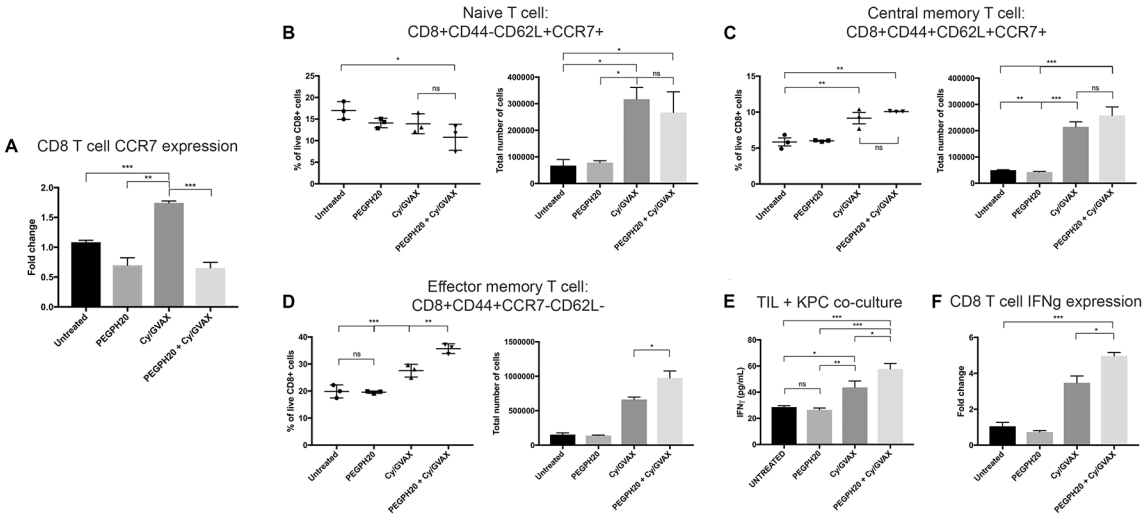

Figure 4. Modulation of CXCL12/CXCR4/CCR7 axis by PEGPH20 in combination with GVAX is associated with increased number of effector memory CD8$^+$ T-cells with enhanced antitumor IFNγ secretion and expression.

Following hemispleen implantation of KPC cells, tumor-bearing mice were treated with Cy (100 mg/kg) on Day 6, PEGPH20 (40μg/kg) on Day 6 and GVAX on Day 7. Mice were sacrificed on Day 16. (**A**) CD8$^+$ cells were isolated from tumor infiltrating lymphocytes (TIL) by negative selection and RNA extracted (n=3 mice). qPCR reveals patterns of CD8$^+$ cell CCR7 expression in single agent treatment and combination treatment groups. Flow cytometry was performed on TIL isolated from processed murine liver in 3 mice analyzed individually. Histograms show the percentage and total number of live (**B**) naïve T-cells as identified by the markers: CD8$^+$CD44$^-$CD62L$^+$CCR7$^+$, (**C**) central memory T-cells: CD8$^+$CD44$^+$CD62L$^+$CCR7$^+$ and (**D**) effector memory T-cells: CD8$^+$CD44$^+$CCR7$^-$CD62L$^-$. (**E**) ELISA assays were performed to assess IFNγ secretion of isolated CD8$^+$ T-cells in each treatment group (n=5 mice pooled). Autologous irradiated KPC tumor cells were utilized as antigenic targets and cocultured with CD8$^+$ T-cells isolated from TIL by negative selection. (**F**) qPCR reveals IFNγ expression in CD8$^+$ cells isolated from tumor infiltrating lymphocytes by negative selection (n=3 mice). Data represent mean ± SEM from one representative experiment that was repeated twice. *ns* not significant, * p<0.05,** p<0.01, ***p<0.001.

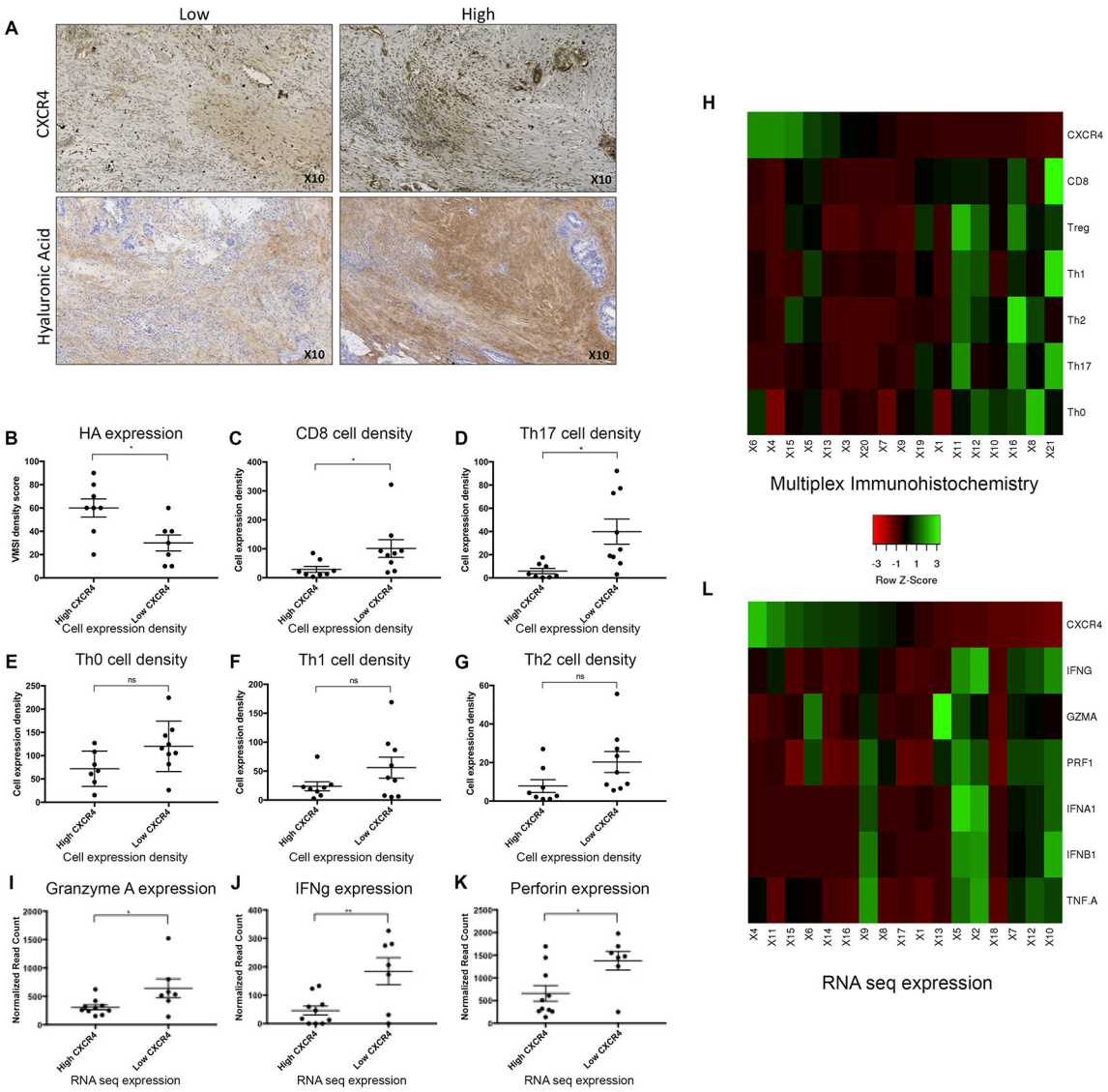

Figure 5. Relationships of hyaluronan and the CXCR4 axis are appreciated in human PDAC in the setting of GVAX.

Human PDAC tissue were collected from patients after one dose of neoadjuvant GVAX and subsequent surgical resection at our institution (n=22). (**A**) Immunohistochemistry (IHC) staining of CXCR4 (n=17) and hyaluronan (HA) expression was performed (n=15). (**B**) Analysis of HA expression in GVAX treated PDAC tumor with high stromal CXCR4 expression compared to tumor with low CXCR4 expression by IHC. The percentage of total cell subsets, as determined by multiplex IHC, were compared between high vs low CXCR4 expression groups: (**C**) $CD8^+$ T-cells: $[CD45^+CD3^+CD8^+]$ (**D**) $Th17^+$ T-cells: $[CD45^+CD3^+CD8^+Foxp3^-RORlt^+]$ (**E**) Th0: $[CD45^+CD3^+CD8^-Foxp3^-RORgt^-Tbet^-GATA3^-]$ (**F**) Th1: $[CD45^+CD3^+CD8^-Foxp3^-RORgt^-Tbet^+]$ (**G**) Th2: $[CD45^+CD3^+CD8^-Foxp3^-RORgt^-GATA3^+]$. (**H**) Heat map generated to visualize the relationship of protein expression of CXCR4 and the density of immune cell infiltrates, particularly $CD8^+$ T-cells, according to the quantification of IHC results. Whole exome RNA

sequencing was performed on dissected pancreatic stroma of the same cohort of patients (n=17). (**H**) Granzyme A (**I**) IFNγ and (**J**) Perforin expression in PDAC tumor with high stromal *CXCR4* expression were compared to tumor with low *CXCR4* expression. (**K**) Heat map generated to visualize the relationship between the RNA expression of *CXCR4* and the expression of markers of effector T-cell function. Data represent mean ± SEM. *ns* not significant, * $p<0.05$,** $p<0.01$

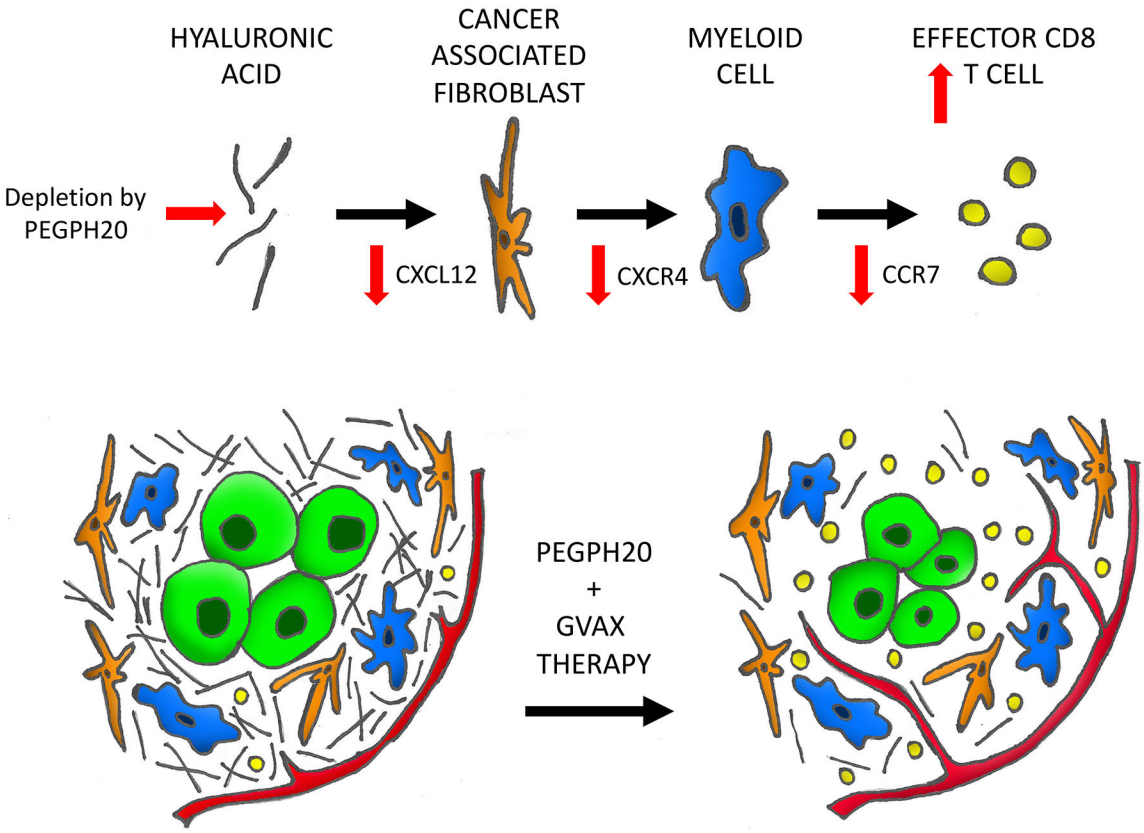

Figure 6. A working model of the mechanistic role of PEGPH20 in the microenvironment of PDAC.

The pancreatic cancer tumor microenvironment is dense, fibrotic and excluded from immune surveillance leading to a paucity of CD8 T-cells. PEGPH20 targets and depletes the extracellular matrix hyaluronic acid allowing vascular expansion and access to the tumor. An associated decrease in CXCL12 expression is appreciated in the cancer associated fibroblasts within the stroma. Downstream CXCR4 expression is diminished in the myeloid cells. CCR7 expression is then decreased in infiltrating CD8 cells leading to a skew towards the effector memory T-cell subtype.